

Supporting Information

Optimized photoluminescence of red phosphor $\text{K}_2\text{TiF}_6:\text{Mn}^{4+}$ synthesized at room temperature and its formation mechanism

Lifen Lv, Zhen Chen, Guokui Liu, Shaoming Huang, and Yuexiao Pan*

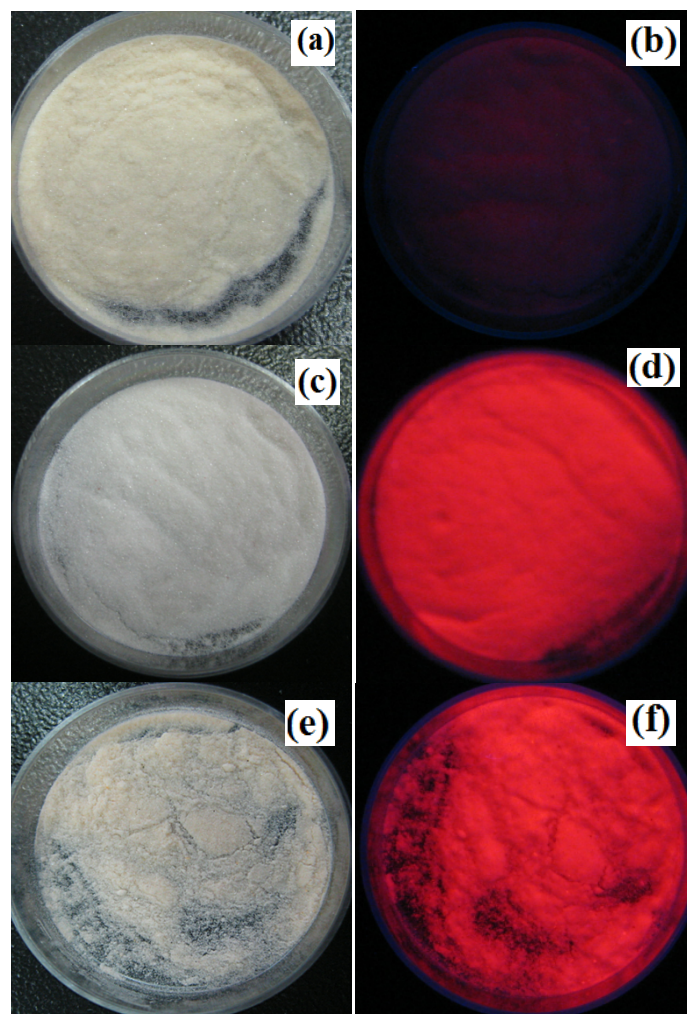


Figure S1. Photographs of the phosphor samples (a,b) KTFM-1, (c,d) KTFM-2, and (e,f) KTFM-3 (prepared according to the detailed experimental process as described in Table 1) under (a,c,e) visible light and (b,d,f) 365 nm UV light excitation, respectively.

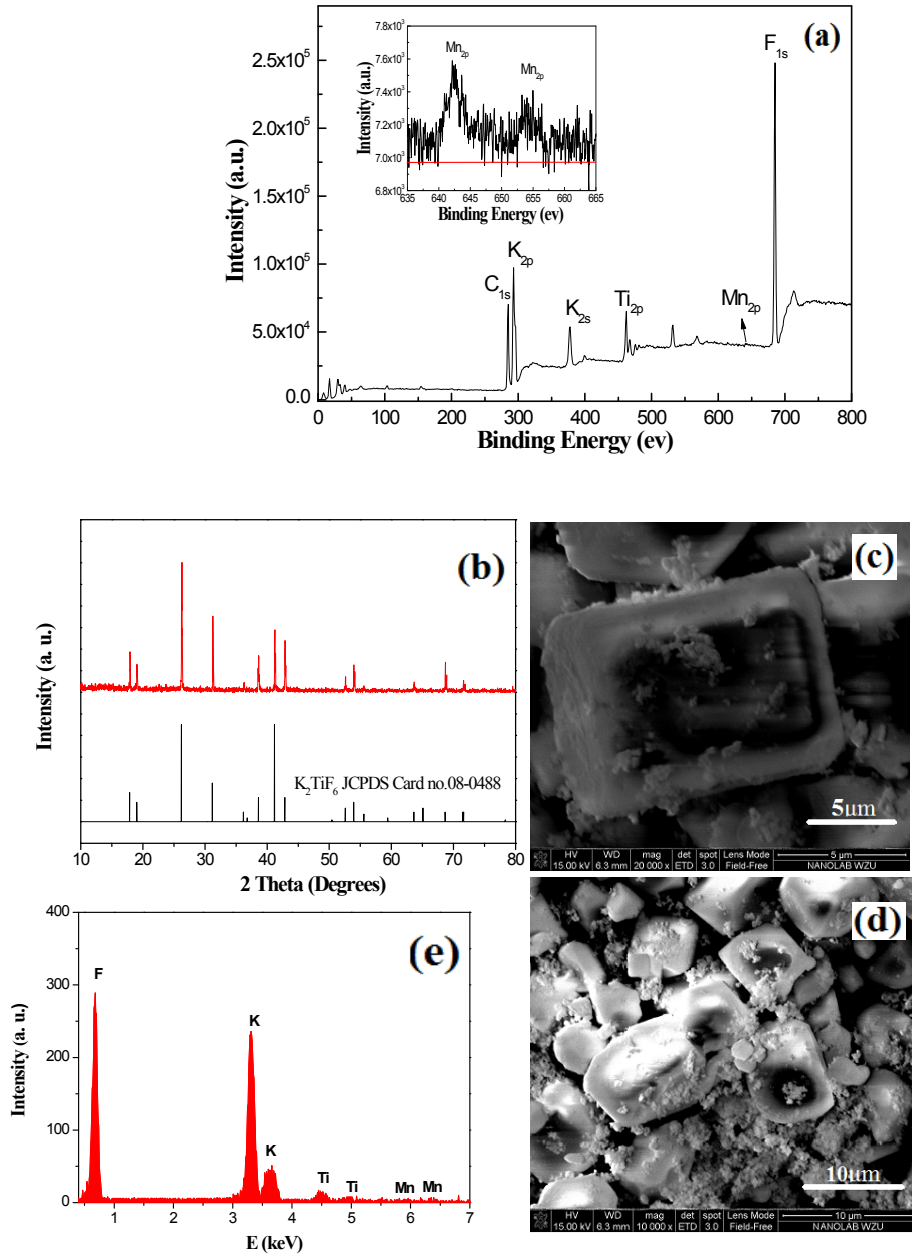


Figure S2. (a) X-ray photoelectron spectroscopy (XPS) of $\text{K}_2\text{TiF}_6:\text{Mn}^{4+}$ prepared by from $\text{Ti}(\text{OC}_4\text{H}_9)_4$. (b) XRD, (c,d) SEM images, and (e) EDS spectrum of red phosphor $\text{K}_2\text{TiF}_6:\text{Mn}^{4+}$ prepared from TiO_2 .

Note: XPS spectrum was obtained with a PHI 5000 (ULVAC-PHI, Chigasaki, Kanagawa, Japan) system equipped with a 450 W monochromatic Al $K\alpha$ X-ray under ultra-high vacuum.

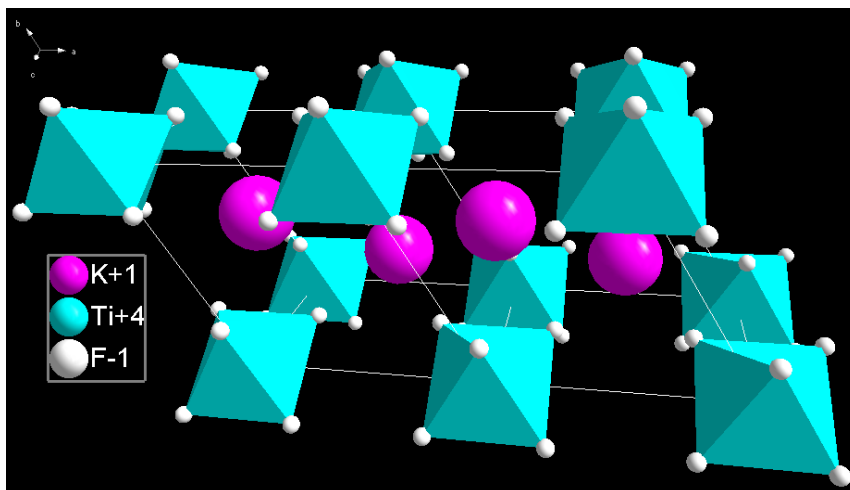


Figure S3. The structure projection of K_2TiF_6 with hexagonal structure plotted by software Diomand 3.0.

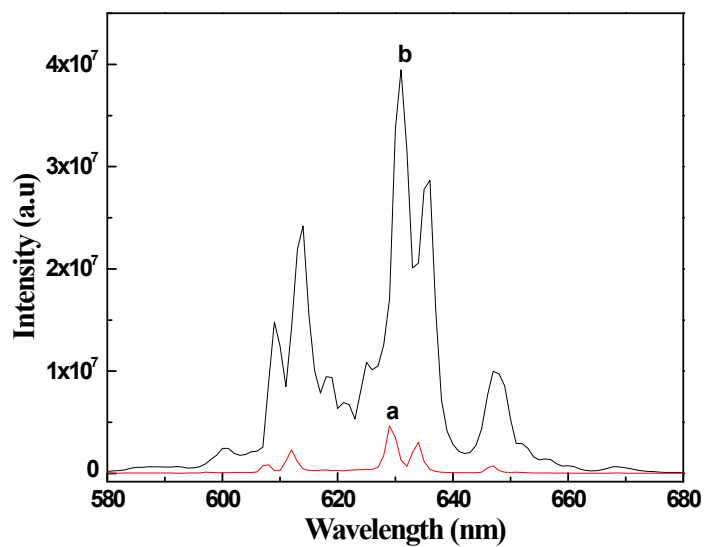


Figure S4. Emission spectra of red phosphors $K_2TiF_6:Mn^{4+}$ prepared by etching (a) TiO_2 and (b) $Ti(OC_4H_9)_4$, respectively. Note: all the other experimental parameters are identical for both synthetic techniques.

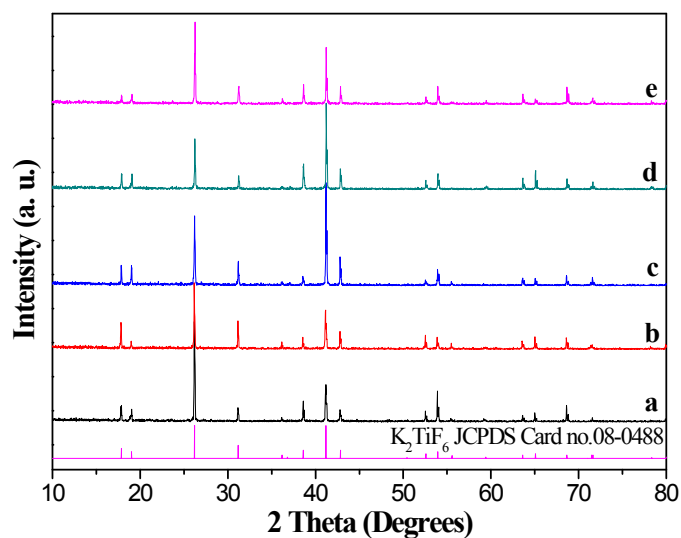


Figure S5. XRD patterns of red phosphors $\text{K}_2\text{TiF}_6:\text{Mn}^{4+}$ prepared by wet chemical etching at room temperature with concentration of KMnO_4 at (a) 0, (b) 5, (c) 10, (d) 25, (e) 30, (f) 60 mmol.L^{-1} .

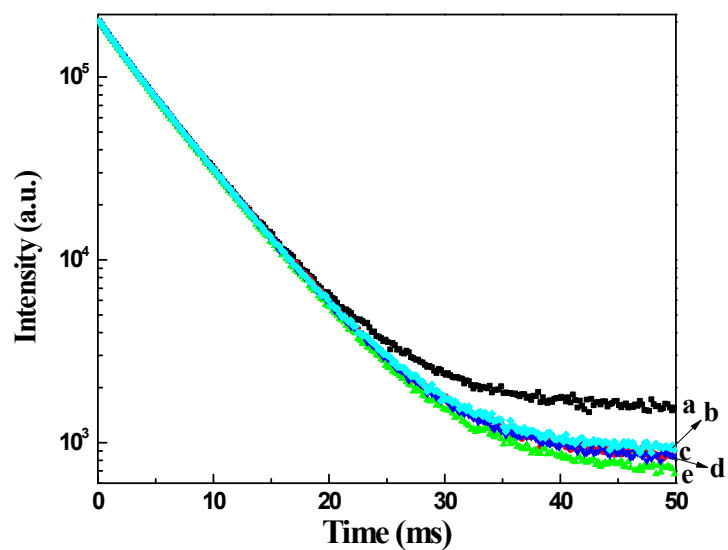


Figure S6. Decay curves of red phosphors $\text{K}_2\text{TiF}_6:\text{Mn}^{4+}$ prepared by wet chemical etching at room temperature with concentration of KMnO_4 at (a) 0, (b) 5, (c) 10, (d) 25, (e) 30, (f) 60 mmol.L^{-1} .

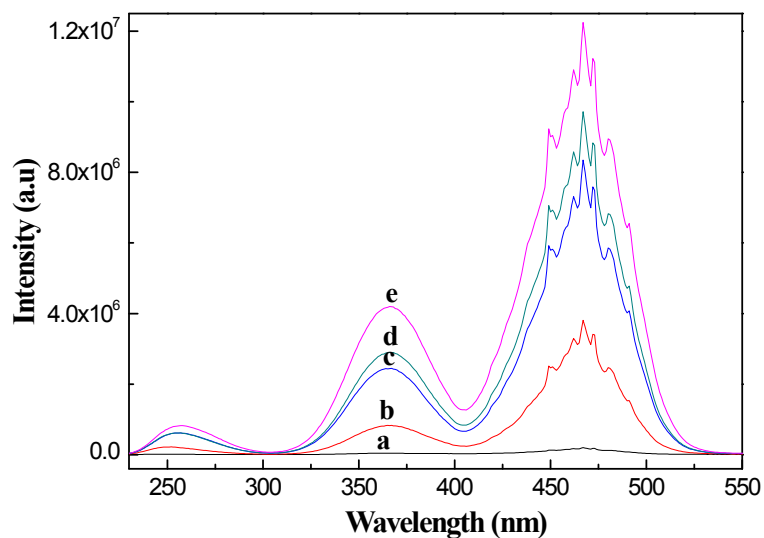


Figure S7. Excitation spectra (monitored at 631 nm) of red phosphors $\text{K}_2\text{TiF}_6:\text{Mn}^{4+}$ prepared by wet chemical etching at room temperature with concentration of HF at (a) 5, (b) 10, (c) 20, (d) 30, (e) 40 wt.%.

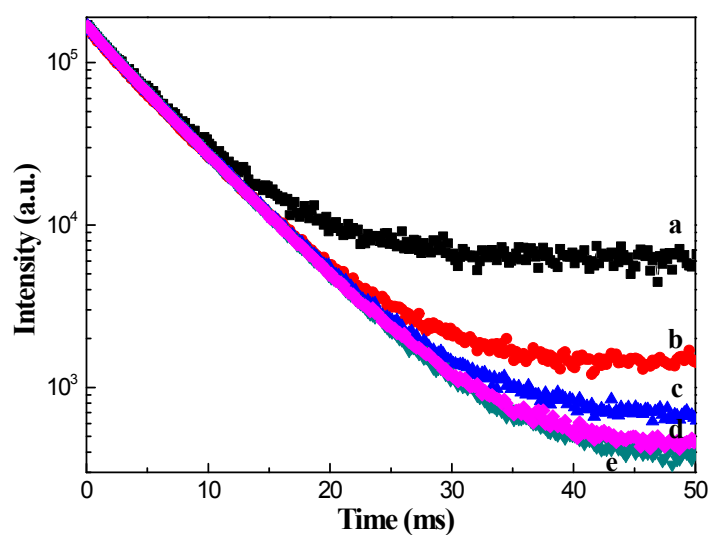


Figure S8. Dependence of decay of 631 nm emissions of red phosphor $\text{K}_2\text{TiF}_6:\text{Mn}^{4+}$ (excited at 467 nm) prepared with concentration of HF at (a) 5, (b) 10, (c) 20, (d) 30, (e) 40 wt.%.

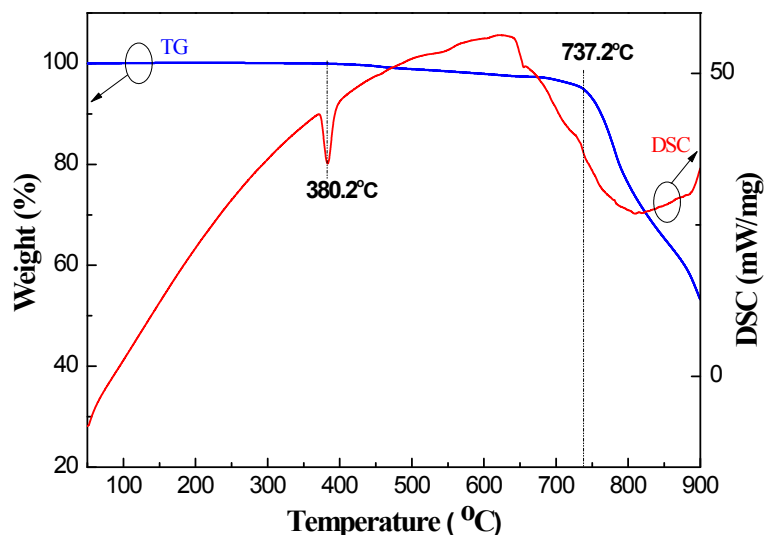


Figure S9. Thermogravimetrics (TG) and different scanning calorimeter (DSC) graphs of as synthesized $\text{K}_2\text{TiF}_6:\text{Mn}^{4+}$ under N_2 atmosphere. The thermal stability the red phosphor behavior of $\text{K}_2\text{TiF}_6:\text{Mn}^{4+}$ is investigated by thermogravimetrics analysis and different scanning calorimeter (DSC; Netzsch STA 449 C, at a heating rate of 10K/min). (The data are repeatable).

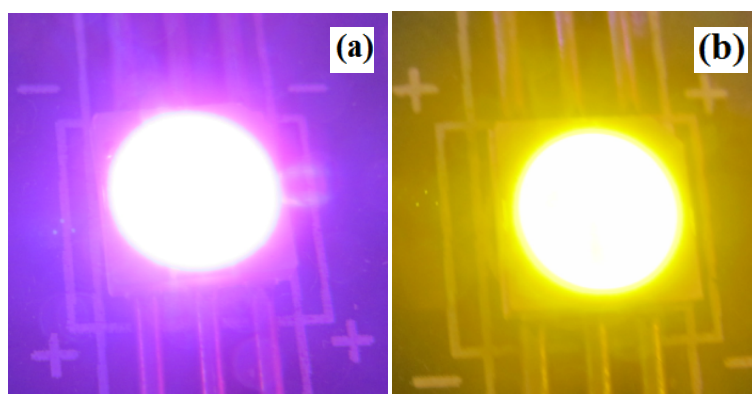


Figure S10. Photographs of (a) purple LED fabricated with $\text{K}_2\text{TiF}_6:\text{Mn}^{4+}$, and (b) "warm" white LED fabricated with $\text{K}_2\text{TiF}_6:\text{Mn}^{4+}$ and $\text{YAG}:\text{Ce}^{3+}$ driven at under 60-mA current. The LEDs were examined by a LEE300E UV-Vis-near IR spectrophotometer (Everfine photo-E-Infor Co., China).